Sensorless Predictive Current Control of Multiphase Buck Converter for MPPT Application

By

Muhammad Umar Abbasi

(Registration No: 00000364407)

Department of Electrical Engineering

School of Electrical Engineering and Computer Science

National University of Sciences & Technology (NUST)

Islamabad, Pakistan

(2024)

Sensorless Predictive Current Control of Multiphase Buck Converter for MPPT Application

By

Muhammad Umar Abbasi

(Registration No: 00000364407)

A thesis submitted to the National University of Sciences and Technology, Islamabad,

in partial fulfillment of the requirements for the degree of

Master of Science in
Electrical Engineering

Supervisor: Dr. Jawad Arif

School of Electrical Engineering and Computer Science

National University of Sciences & Technology (NUST)

Islamabad, Pakistan

(2024)

THESIS ACCEPTANCE CERTIFICATE

Certified that final copy of MS/MPhil thesis entitled "Sensorless Predictive Current Control of Multiphase Buck Converter for MPPT Application" written by Muhammad Umar Abbasi, (Registration No 364407), of SEECS has been vetted by the undersigned, found complete in all respects as per NUST Statutes/Regulations, is free of plagiarism, errors and mistakes and is accepted as partial fulfillment for award of MS/M Phil degree. It is further certified that necessary amendments as pointed out by GEC members of the scholar have also been incorporated in the said thesis.

Signature: _____

Name of Advisor: ____Dr. Jawad Arif_____

Date: _____28-Mar-2024_____

HoD/Associate Dean:_____

Date: _____28-Mar-2024_____

Signature (Dean/Principal): _____

Date: _____28-Mar-2024_____

FORM TH-4

National University of Sciences & Technology

MASTER THESIS WORK

We hereby recommend that the dissertation prepared under our supervision by: (Student Name & Reg. #)___Muhammad Umar Abbasi [364407]___

Titled: Sensorless Predictive Current Control of Multiphase Buck Converter for MPPT Application

be accepted in partial fulfillment of the requirements for the award of ___Master of Science (Electrical Engineering)___ degree.

Examination Committee Members

1. Name: Usman Ali   Signature: _Usman Ali_
                                                        27-May-2024 1:39 PM

2. Name: Sajjad Hussain   Signature: _Sajjad_
                                                        27-May-2024 1:39 PM

Supervisor's name: Jawad Arif   Signature: _____
                                                        27-May-2024 4:27 PM

_____   29-May-2024
Salman Abdul Ghafoor   _____
HoD / Associate Dean   Date

COUNTERSINGED

___29-May-2024___   _____
Date   Muhammad Ajmal Khan
                                    Principal

THIS FORM IS DIGITALLY SIGNED

AUTHOR'S DECLARATION

I <u>Muhammad Umar Abbasi</u> hereby state that my MS thesis titled "<u>Sensorless Predictive Current Control of Multiphase Buck Converter for MPPT Application</u>" is my own work and has not been submitted previously by me for taking any degree from National University of Sciences and Technology, Islamabad or anywhere else in the country/ world.

At any time if my statement is found to be incorrect even after I graduate, the university has the right to withdraw my MS degree.

Name of Student: <u>Muhammad Umar Abbasi</u>

Date: <u>31-5-2024</u>

DEDICATION

This thesis is dedicated to my beloved parents, my loving wife and our

beloved daughter

ACKNOWLEDGEMENTS

The author would like to acknowledge the sincere efforts and dedication of the faculty at SEECS which provided him with guidance and encouragement during the course of his studies. Especially I would like to thank Dr. Ammar Hassan for his encouragement and belief in my abilities to carry out my work. I would also like to thank Dr. Jawad Arif for his help and encouragement during the completion phase of this thesis. I would also like to thank my committee members, Dr. Usman Ali and Dr. Sajjad Hussain, for being kind and generous in their assessment of my work.

TABLE OF CONTENTS

LIST OF TABLES

LIST OF FIGURES

LIST OF SYMBOLS, ABBREVIATIONS AND ACRONYMS

MPPT   Maximum Power Point Tracking

PV   Photo Voltaic

SPCC   Sensorless predictive current control

CC-CV   Constant Current – Constant Voltage

ADC   Analog to Digital Converter

PWM   Pulse width modulation

ABSTRACT

The commercial MPPT solar charge controllers are mostly single phase buck converters which take the power from solar panels and charge the battery bank connected at the output as well as provide power to the DC loads. As the current rating of these converters increases, the size of the magnetics element also increases which increase the overall cost and weight of the converter. In order to make the converters small in size and weight yet deliver high output current, a multiphase buck converter is envisioned to be used in MPPT solar charge controller applications. Multiphase buck converters have several advantages over single phase versions, such as small inductor size, small output current ripple and improved efficiency. This works describes the development of a sensorless current control strategy for a multiphase buck converter. The sensorless current control eliminates the need for costly current sensors. The current of each phase of multiphase buck converter is estimated and the estimated value is used to control the current of the converter. The current estimation and current control algorithms are based on predictive current control theory. The model of the power stage of the converter is used to derive the current estimation and current control

equations. Furthermore, the current estimation and control equations are derived for single phase buck versions and then seamlessly expanded to the four phase versions. It is shown that this is indeed possible and simulation results are presented to corroborate the theoretical working. The equations are derived in discreet domain and are tailored for implementation on a digital controller such as STM32G474 device. The proposed current sensorless approach is implemented and simulated in MATLAB/SIMULINK environment. The results obtained affirm the usefulness of current sensorless approach. A hardware prototype setup is attempted for the implementation of the proposed sensorless current control of the multiphase buck converter. The development of this hardware prototype as well as the issues encountered are also discussed.

CHAPTER 1: INTRODUCTION

1.1 Background

In the modern age, electricity generation and utilization has become a central issue in the development and progress of a nation. As such, the sources used to generate the electric energy are increasingly being scrutinized for their impact on the environment. To this effect, less fossil fuel based and more renewable energy based sources are being preferred all over the world in order to reduce the carbon dioxide emissions. Solar energy is increasingly being incorporated in the energy mix of the nations around the world because of its abundance and ease of utilization. The power electronic systems used to process and utilize the solar energy are also getting more and more attention. A plethora of solar charge controllers available in the market are a major indicator of this trend. The most common form of power electronic system used to process solar energy are buck converters. Commercially available DC/DC converters are mostly of single phase buck type. Buck converters take energy from PV arrays and charge batteries used for storage as well as directly supply DC loads. At high power levels, the size of magnetic element in single phase buck converters become prohibitively large. The cost of magnetic element also rises sharply in proportion to its size. A straight forward solution to the above mentioned problem is to split one large inductor into many smaller sized inductors. This results in the formation of multiphase buck converters. A multiphase buck converter is essentially a combination of multiple single phase buck converters that share input and output ports and are operated in a relative phase shift to each other. The advantages of multiphase buck converters over their single phase counterparts include reduced magnetic size, smaller current and voltage ripples at the output of the converter and improved overall efficiency. Moreover, the transient response of the multiphase buck converters is also superior because of smaller effective inductance. The multiloop control of DC/DC converters is a traditional control method in which two loops, one inner current control loop and one outer voltage control loop, are utilize to achieve the control objectives. The current control loop controls the current flowing through the magnetic element of the converter and receives its reference point from the outer voltage loop. The outer voltage loop controls the output or the input

1

voltage of the converter. This method essentially decouples the two loops thus resulting in ease of designing the respective loops. The control of multiphase buck converters is relatively difficult due to increased complexity of the power processing stage. Multiloop control structures are thus very suitable to control multiphase buck converters. Digital control has increasingly been incorporated in the power electronics because of its advantages over traditional analog control systems. Few advantages of digital control are its immunity to component aging and tolerances, implementation of sophisticated control techniques and ability to change the control algorithm by software modification. Multiloop control structures can also be easily implemented inside a digital processor. Due to these reasons, digital implementation of control structures is explored in this work.

Current control of power electronic systems requires sensing of current flowing through the magnetic element. This in turn requires costly current sensors which can increase overall system cost and complexity. Moreover, in case of a multiphase buck converter, implementing current control would entail current sensor for each phase. This can become prohibitive if the number of phases becomes large. These issues make sensorless current control a very suitable strategy for controlling multiphase buck converter. The overall block diagram of the system is presented next in **Figure 1.1**.1:
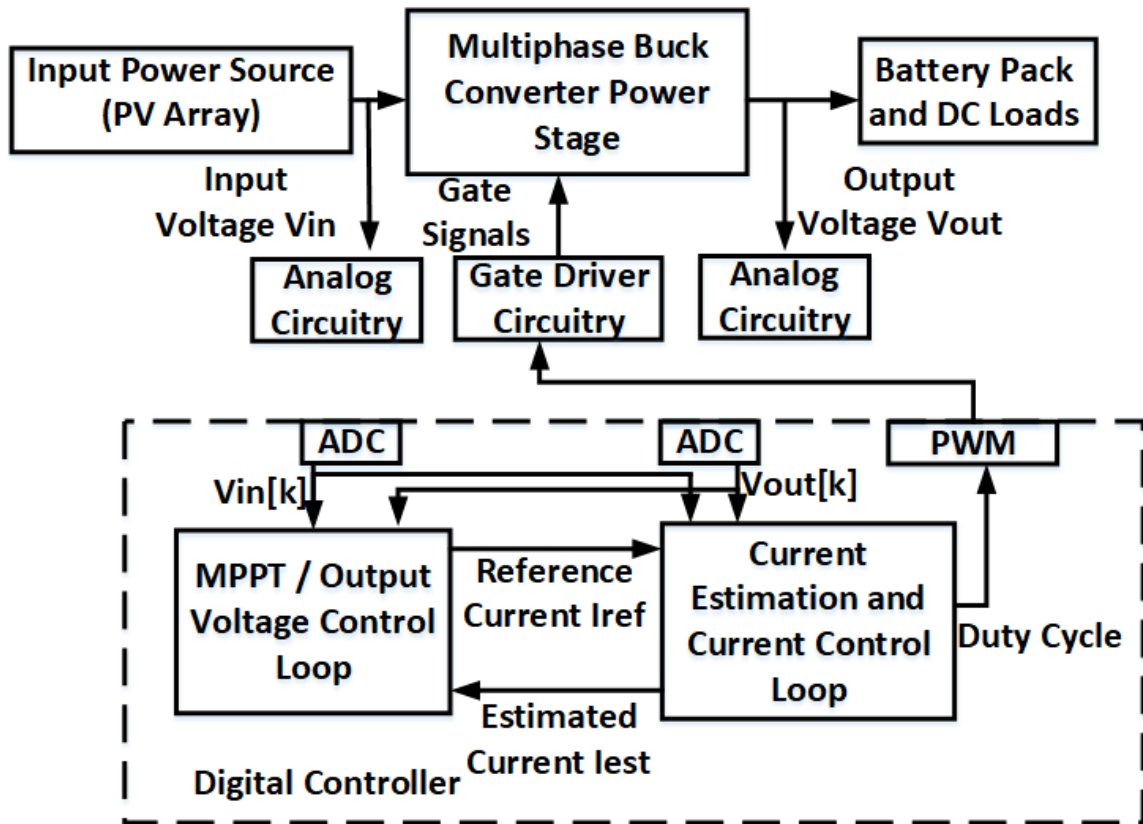
Figure 1.1 System Block Diagram

The power stage of the multiphase buck converter is interfaced with the digital controller through the analog circuitry and the gate driver circuitry. The analog circuits are used to scale the input and output voltages within the range of the controller ADCs. The output of the digital controller is the PWM gate signals which are interfaced to the gate driver circuitry. The gate drivers are used to drive the gates of the physical MOSFET devices. The dual loop control system is implemented inside a digital controller i.e. STM32G474 device.

In dual loop control structure, the MPPT/ voltage control loop is the outer control loop which regulates the input solar power or the output battery voltage and current. The outer loop sets the reference value of the current for the inner current control loop. The inner current control loop has two objectives: to estimate the current flowing through the inductors of the multiphase buck converter and then control the estimated currents using the predictive current control law.

3

1.2 Problem Statement

To develop a simple sensorless current control strategy for a multiphase buck converter. The strategy should be simple enough to be implemented on a low cost micro-controller in digital domain. The multiphase buck converter should be suitable for use in MPPT charge controller applications.

1.3 Research Motivation

Commercially available solar charge controllers are of single phase buck type. The size of the magnetic element becomes very large as the power rating of the converter increases. This increases overall converter size, weight and cost. In order to reduce the size of the magnetic element thereby improving overall converter size, weight and cost, multiphase buck converter topology should be explored for this application area. Multiphase topology has better performance in terms of improved current and voltage ripple at the converter output. The sensorless current control should be employed for the multiphase buck converter to make it commercially viable in the market.

1.4 Research Objectives

To develop a sensorless current control strategy for a four phase buck converter based on model predictive current estimation and current control. The said strategy should be simple enough to be implemented on a low cost platform such as STM32G47 microcontroller. To develop a hardware prototype for implementation of the sensorless current control strategy for four phase buck converter.

1.5 Thesis Organization

The thesis has organized as follows:

Chapter 2 focuses on the literature review for the work presented in this thesis. Major focus has been placed on exploring the work done on sensorless current control,

particularly model predictive based current estimation and current control. A brief overview of MPPT techniques and battery charging methods is also presented.

Chapter 3 explains the mathematical modelling of the sensorless current estimation. The mathematical modelling is carried out in discreet time domain. The modelling of the single phase buck is extended to the four phase buck converter. The effect of elements on the current estimation convergence is explored and brief simulation results are presented to corroborate the theoretical analysis.

Chapter 4 presents the current control of the four phase buck converter. The model predictive current control of a single phase buck converter is used as a basis and is further extended to four phase buck converter. The controlled parameter is the estimated current obtained from the current estimation. It is shown that the predictive current control effectively controls the currents flowing through the inductors of the multiphase buck converter

Chapter 5 presents the MPPT tracking algorithm implementation and battery charging control. The MPPT algorithm employed in this work is perturb and observe based algorithm which is widely used in the industry because of its simple implementation and high reliability. The battery charging control method adopted in this work in constant current- constant voltage (CC-CV) charging method. This method is used for charging state of the art Lithium Ion batteries and is very simple and effective method of battery charging control.

Chapter 6 presents the simulation of the proposed four phase buck converter and its control algorithm in MATLAB/ SIMULINK environment. The power stage and control system are implemented and simulated and the simulation results are used to verify the effectiveness of the sensorless current control. MPPT tracking control loop as well as battery charge control are also demonstrated in simulation.

Chapter 7 presents the work done in an attempt to develop a prototype of the four phase buck converter. The progress achieved, issues encountered as well as future plan of work

are discussed. The implementation of the current estimation and current control algorithm on STM32G474 device are also discussed.

1.6 Thesis Contributions

In this work, a sensorless current control strategy for a multiphase buck converter is studied and developed. The current estimation is performed using mathematical model of the buck converter. The current estimation equation is derived for the single phase buck converter. Then the method is extended to the multiphase buck converter version. Model predictive current control strategy is employed to control the estimated current. The structure of the current estimation and current control equations are shown to be very similar. Both the current estimation and current control equations are derived in discreet time domain which is suitable for the digital implementation on a digital controller. The aforementioned current estimation and current control strategies are simulated for a four phase buck converter which is employed for MPPT and battery charging applications. The simulation of the system is carried out in MATLAB/ SIMULINK environment and simulation results are presented to verify the theoretical work. A hardware prototype is also developed and its progress is presented in this thesis. The issues encountered in the working of the hardware prototype are discussed and the outline of future work is presented.

CHAPTER 2: LITERATURE REVIEW

The focus of this work is on the sensorless current control of a multiphase buck converter. The converter is targeted for MPPT tracking solar battery charging applications. The literature review for this work is divided into three major sections: first section is dedicated to the literature review of the existing techniques used to estimate the inductor current in a dc/dc converter. The next section will focus on the current control techniques for dc/dc converters presented in the literature. Final section of this chapter will briefly review the MPPT tracking methods commonly used in the industry as well as battery charging control methods used for lead acid and lithium ion batteries employed in residential and industrial applications.

2.1 Current Estimation Techniques

The sensorless current estimation can be traced back to [1]. The author presented an approach in which inductor voltage is integrated to obtain the inductor current. However, this technique is not suitable for digital implementation. In [2], author presents an observer based approach for estimating the inductor current. However, this technique suffers from low accuracy and doesn't include the effect of the converter parasitics such as series resistance of devices and magnetics on the convergence of the estimated current. In [3] and [4], extended Kalman filter based approaches are presented in order to estimate the current flowing through the magnetics of the converter. However, these approaches are complex and require high computation capabilities and thus not suitable for implementation on a low cost microprocessor. In [5], a Luenberger Observer is applied to a dc/ dc converter to estimate the inductor current. However, this work doesn't consider the parasitics of the converter and its convergence is not guaranteed in the real converter. In [6], the authors present a method for estimating the average inductor current in dc/ dc converters. This method measures the switch node voltage in order to calculate the inductor voltage and estimate inductor current. An extra voltage sensor is thus required for measuring node voltage. This becomes disadvantageous in case of a multiphase buck converter as an additional sensor would be required for each phase. In [7], a sensorless equal current

sharing technique is presented for a two phase buck converter. The current is equally divided among two phases without knowing actual current value. In [8], a logarithmic current sharing method is described for multiphase dc/ dc converters. The method is very complex and not suitable for implementation on a low cost controller. Moreover, the converter current is not estimated. In [9], sensorless current sharing for multiphase converters is presented. This method forces equal current sharing without actual current estimation. The aforementioned methods of equal current sharing for multiphase converters suffer from complexity and lack of actual current estimation value. In [10], [11], prediction based current estimation methods are presented. These methods use the mathematical model of the dc/ dc converter to predict the current of the inductor at the next switching cycle. These methods are implemented in discreet domain and can be easily tailored for implementation on a low cost commercial microcontroller. In this work, a simple first order digital filter based current estimator is employed which is derived from works in [10], [11]. In the next chapter, the derivation of the current estimation equations is carried out. The current estimator is then extended to four phase version and simulation results are presented.

2.2 Current Control Techniques

Many techniques have been reported in the literature for current control of dc-dc converters. Starting from simple PI controller in [12] used to control current of a dc-dc converter. PI controllers can be easy to implement but their performance may be inadequate for complex systems like multiphase buck converter. In [13] a hysteresis based current controller has been presented for cube sat applications. Hysteresis current controllers are effective in controlling switching converters, but they suffer from variable switching frequency. In [14], comparison of type2 and type 3 controller for the current control of dc-dc converters has been presented. The derivation of controller parameters for complex systems such as multiphase buck converter can become difficult. In [15], sliding mode control has been applied for the current control application. However, derivation of sliding surface and chattering issue makes this control technique not simple for implementation. In [16], proportional resonant current controller is applied for the current control of a grid connected inverter. This type of current controller is more suitable for varying reference

application such as those in grid tied converters. Fuzzy logic and neural network based controller has been presented in [17], however this type of controller is not suitable for implementation on a low cost microcontroller. Model predictive control has found wide spread application in the control of switching converters in recent years. In [18] and [19], model predictive control is applied to the dc-dc converter. The calculation of cost function and its minimization steps can be computation intensive for some applications. In this work, model predictive based deadbeat current control is adopted which was originally presented in [20]. It will be shown in subsequent chapter that this is simplest possible control law as it is derived directly from the mathematical modelling of the switching converter. The implementation of the current control is very straight forward on a digital system such as a microcontroller. Moreover, it will be shown that the extension of single phase version to four phase version is very easy and straight forward.

2.3 MPPT Techniques and Battery Charging Control

In this section, a brief review will be carried out of the important techniques reported in literature for the MPPT of the solar arrays as well charging control methods for batteries. In [21], a constant voltage based method is presented for tracking MPPT. This method is based on assumption that the ratio between maximum point voltage (Vmp) and open circuit voltage (Voc) is approximately 0.78. The PV array voltage is regulated to a reference value which in turn tracks the maximum power point. In [22], a hill climbing method is experimentally explored for MPPT applications. In this method, PV power is recorded at an initial operating point of the converter. Then the slope of power and voltage curve is calculated to determine the direction of next perturbation. At the maximum power point, the slope of the p-v curve is very close to zero. Incremental conductance based MPPT algorithm is presented in [23]. In this method, the impedance of the PV array source is matched to that of the power converter by changing the operating point of the converter. When both impedances are matched, maximum power is transferred from PV array to the converter. Apart from these, ripple correlation method has been presented in the literature for MPPT tracking applications in [24]. In this method, the sign of the PV power and voltage curve slope is used to determine the direction of the perturbation. At maximum power point, the slope of power and voltage curve is zero. Apart from these traditional

9

methods, other approaches such as artificial neural network based and global search optimization based methods have also been explored in the literature for finding the maximum power point of the PV array. However, these methods are not suitable for low cost applications and thus not considered here. In this work, hill climbing method is used to implement the MPPT algorithm because of its wide spread use in the industry and its ease of practical implementation. In literature, many charging schemes have been presented which are suitable for different battery management applications. For example, [25], nickel type batteries need to be charged using only constant current scheme. On the other hand, Li-Ion batteries require both constant current as well as constant voltage charging stages. The battery packs that are composed of different cells connected in series also require consideration of individual cell voltage levels. Since the focus of this work is sensorless current control of power converter, for simplicity constant current and constant voltage based charging scheme is adopted for demonstration purposes.

# CHAPTER 3: CURRENT ESTIMATION OF MULTIPHASE BUCK CONVERTER

The multiloop control structure adopted in this work for the control of a four phase buck converter consists of two loops: outer MPPT/ battery charging loop and inner current control loop. The inner current control loop is responsible for controlling the current through the multiphase buck converter and is the focus of this chapter. The current control of a power converter requires measurement of the current flowing through the inductor of the power stage. The current measurement requires breaking of the current path and placing a current sensing element, typically a low value resistor. However, this causes several problems such as heat dissipation and loss of efficiency, measurement noise issues and sensor cost. In order to mitigate the issues involved in the actual sensing of the controlled current, an alternate approach is to estimate or calculate the inductor current. This chapter will first present the mathematical modelling of the buck converter which forms the basis of the current estimation. The current estimation is then extended to the four phase version and it will be shown why it is easily adopted the multiphase version as well.

## 3.1 Mathematical Modelling of Buck Converter
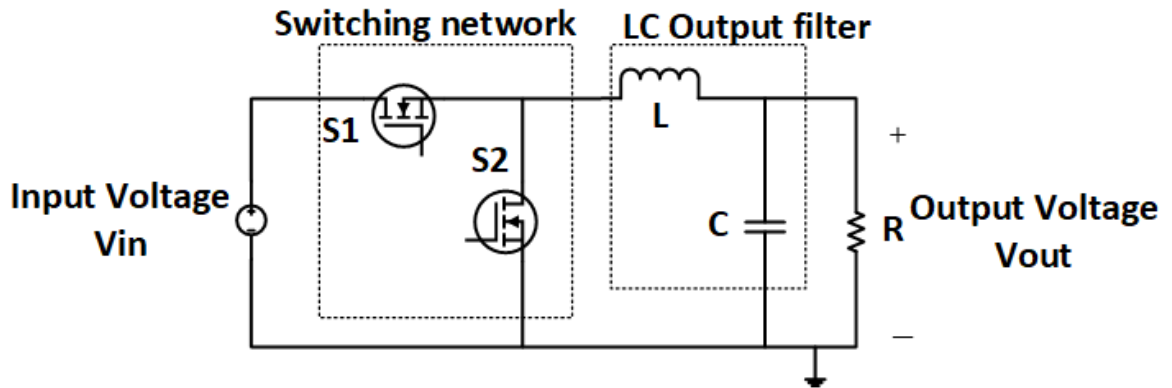
Figure 3.1 Schematic of a single phase Buck Converter

In **Figure 3.1**, the basic schematic of a single phase buck converter is shown. A buck converter is a dc-dc converter which consists of a switching network of two switches S1 and S2 which are operated in complement to each other. This switching network converts input voltage into switching voltage which is passed through output LC filter to obtain output voltage. The magnitude of the output voltage is controlled by controlling the on duration or duty cycle of the switch S1. The major waveforms of the Buck converter are shown next.
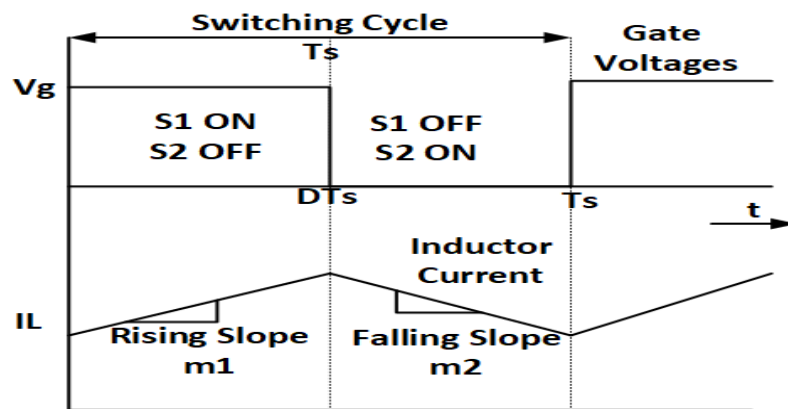
Figure 3.2 Basic Waveforms of a Buck Converter

As can be seen in **Figure 3.2**, the gates of MOSFETS S1 and S2 and turned on in complement to each other during one switching cycle of duration Ts seconds. The switch S1 on time is D*Ts where D is duty cycle of the switch and it is the controlling variable. By changing D, the behavior of the buck converter is controlled. The most important waveform from standpoint of current estimation is the inductor current waveform and it is shown in **Figure 3.2**. The inductor current rises when S1 is ON and inductor current falls when S1 in off. The buck converter schematic is further simplified for each case next and the rising slope of inductor current denoted as m1 and falling slope denoted as m2 are mathematically described.
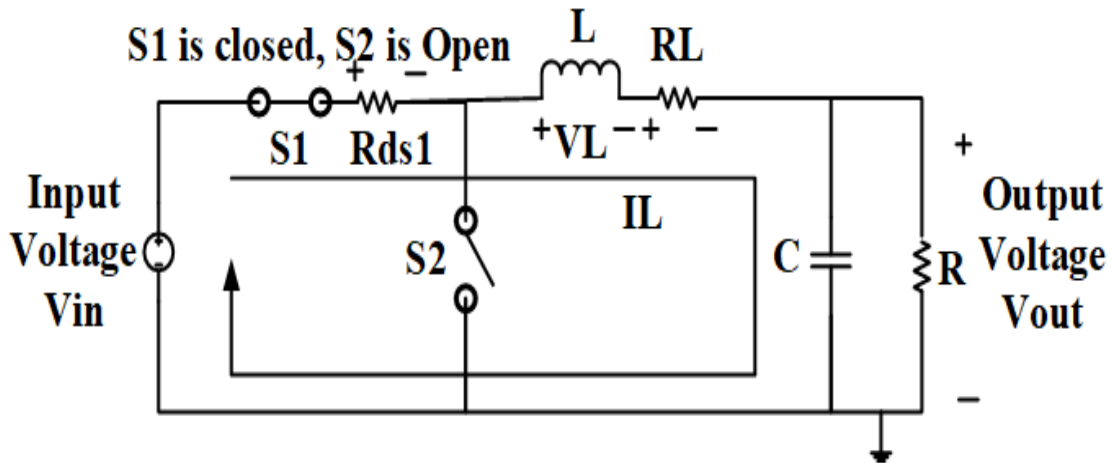
**Figure 3.3** Switch S1 close, S2 open

In **Figure 3.3**, the equivalent circuit of a buck converter during switch S1 on time is presented. It should be noted that the closed MOSFET switch is modeled by a short circuit and an equivalent resistance which is the drain to source resistance of the device. The open MOSFET switch S2 is simply modelled as open circuit. The inductor dc resistance is also included in the circuit since it contributes to the voltage drop in the circuit.

During the time period when switch S1 is close and S2 open, the inductor of the buck converter charges and its current rises. The current flow is from input to the output through the buck inductor. The basic Kirchhoff voltage law around the loop yields the following equation for the voltage across the inductor buck converter.

$$V_L(t) = L * \frac{di(t)}{dt} = V_{in}(t) - I_L(t) * R_{ds1} - I_L(t) * R_L - V_{out}(t) \qquad (3.1)$$

And the rising slope of the inductor can be determined by dividing the Equation 3.1 by inductance L as follows:

$$m_1(t) = \frac{di(t)}{dt} = \frac{V_{in}(t) - I_L(t) * R_{ds1} - I_L(t) * R_L - V_{out}(t)}{L} \qquad (3.2)$$
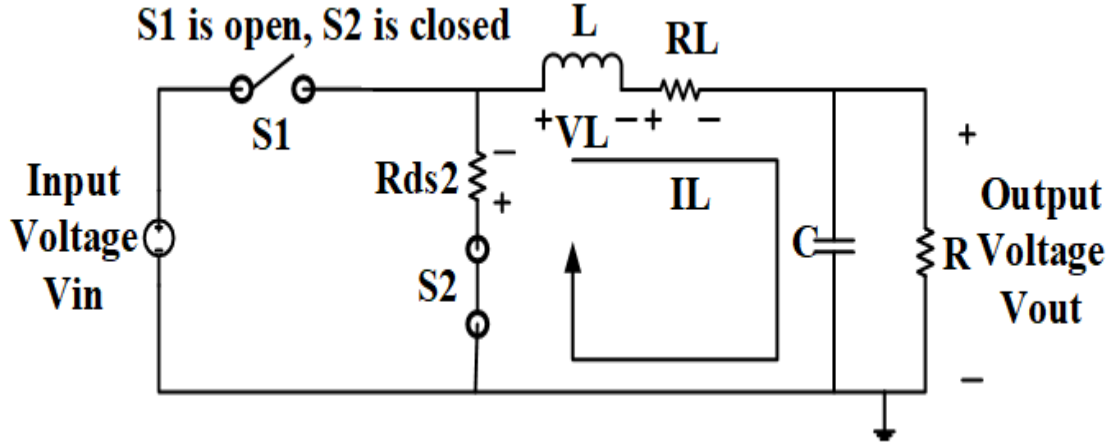
Figure 3.4 Switch S1 open, S2 close

In **Figure 3.4**, the equivalent circuit of the buck converter is shown when the switch S1 is open and S2 is closed. The inductor and the output are disconnected from the input. The inductor discharges and inductor current falls. The voltage around inductor is given as follows:

$$V_L(t) = L * \frac{di(t)}{dt} = -I_L(t) * R_{ds2} - I_L(t) * R_L - V_{out}(t) \qquad (3.3)$$

Likewise, the falling inductor current slope can be determined as:

$$m_2(t) = \frac{di(t)}{dt} = \frac{-I_L(t) * R_{ds2} - I_L(t) * R_L - V_{out}(t)}{L} \qquad (3.4)$$

By inspecting the Equations 3.2 and 3.4, we can conclude that the slopes of the inductor current during the rising and the falling time are dependent on input voltage Vin(t), output

14

voltage Vout(t) as well as the magnitude of the inductor current already flowing through the inductor. The parasitic resistances of the MOSFET switches and the inductor as well as the inductance value itself also shape the slope but these parameters are constant in nature.

The mathematical equations derived for the slopes of inductor current are continuous in nature. In order to implement these equations on a digital system, the equations must be converted into discreet form. The inductor current waveform is reproduced with the focus on the sampling of variables.
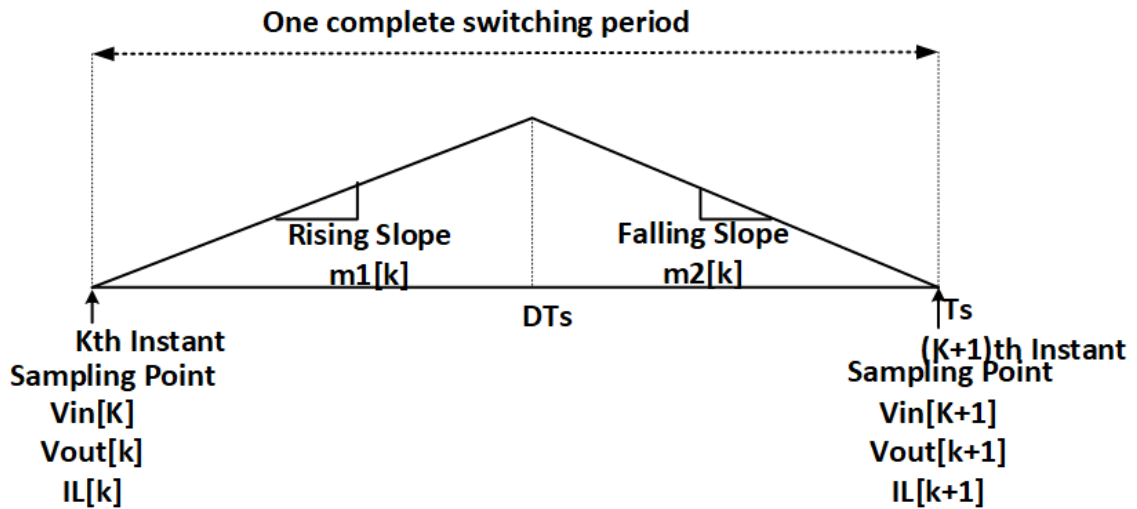
Figure 3.5 Inductor current waveform in one switching cycle

As can be seen in the **Figure 3.5** Inductor current waveform in one switching cycle, the input voltage and the output voltage are sampled at the discreet intervals, specifically when the switch S1 turns on and switch S2 turns off. The rate of sampling of these variables is equal to the switching frequency of the power converter stage. The inductor current samples IL[k] and IL[k+1] are not sampled values rather these are the calculated values available in the digital system. It should be noted that IL[k] is calculated in the previous cycle. Following two assumptions are clarified here:

- The input voltage and output voltage are assumed to be essentially constant during two switching cycles. This is true because in dc/dc converters, the input and output voltages vary very slowly as compared to the switching period of the converter. This implies that Vin[k] ~= Vin[k+1] and Vout[k] ~= Vout[k+1].
- The inductor current is assumed as constant during one switching period. This is true because new value of the inductor current is available after calculation only.

We proceed with the rising slope of the inductor current from Equation 3.2 as follows:

$$m_1[k] = \frac{IL[DTs] - IL[k]}{DTs} = \frac{V_{in}[k] - I_L[k] * R_{ds1} - I_L[k] * R_L - V_{out}[k]}{L} \tag{3.5}$$

Similarly, we discretize the falling slope of the inductor current as follows:

$$m_2[k] = \frac{IL[k+1] - IL[DTs]}{Ts - DTs} = \frac{-I_L[k] * R_{ds2} - I_L[k] * R_L - V_{out}[k]}{L} \tag{3.6}$$

The averaging method of the converter analysis is applied here [26]. The inductor current at instant k+1 is given as follows:

$$IL[k+1] - IL[k] = m1[k] * DTs + m2[k] * D'Ts \tag{3.7}$$

This is because the rising slope is applied for D*Ts time and falling slope m2 is applied for D'*Ts time period. Here D' is the complement of D, i.e. D'= 1-D. We insert the values of the m1[k] and m2[k] in Equation 3.7. Also Rds1=Rds2 since same specification devices are used for both S1 and S2 switches. This leads to following equation:

$$\begin{aligned} IL[k+1] &- IL[k] \\ &= \frac{Vin[k] * DTs - I_L[k] * R_{ds} * Ts - I_L[k] * R_L * Ts - V_{out}[k] * Ts}{L} \end{aligned} \tag{3.8}$$

Further simplification leads to:

$$IL[k + 1] = IL[k] + \frac{Vin[k] * DTs - I_L[k] * R_{ds} * Ts - I_L[k] * R_L * Ts - V_{out}[k] * Ts}{L} \quad (3.9)$$

Equation 3.9 includes the effects of the converter parasitics i.e. the on resistance of the MOSFET switch and dc series resistance of the inductor. We can combine these two parameters into Req and simplify further:

$$IL[k + 1] = IL[k] + \frac{Vin[k] * DTs - I_L[k] * R_{eq} * Ts - V_{out}[k] * Ts}{L} \quad (3.10)$$

Where Req = R_L + $R_{ds.}$

3.2 Extension to Multiphase Version

In the previous section, inductor current estimation equation was derived for a single phase buck converter. In this section, we extend the approach to four phase buck converter version. It will be shown that the same equation derived in Equation 3.10 can be used to estimate the inductor currents of all the phases in a multiphase buck converter. We analyze the inductor current waveforms for a four phase buck converter next.
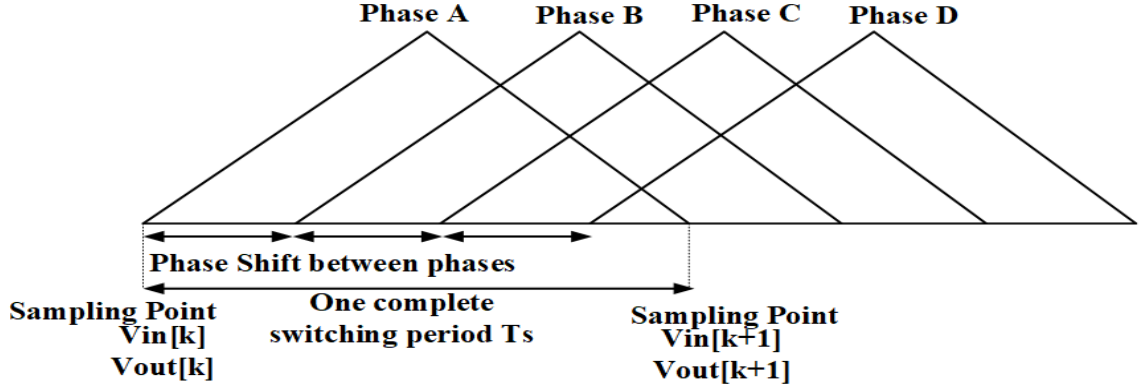
Figure 3.6 Four phase buck converter currents

In **Figure 3.6**, phase currents of a four phase buck converter are shown. The currents are phase shifted with respect to each other within one switching period Ts. As can be seen, the input and output voltages are sampled at the beginning of the switching period only. As such, from the standpoint of the inductor current estimation, the input and output voltages remain constant during one switching period. Therefore, the phase shift between the phases of the multiphase buck converter can be ignored when estimating the inductor currents. The Equation 3.10 is now reproduced for multiphase buck converter.

$$ILn[k + 1] = ILn[k] + \frac{Vin[k] * DTs - I_{Ln}[k] * R_{eqn} * Ts - V_{out}[k] * Ts}{L} \quad (3.11)$$

where n=1,2,3 and 4 for respective phases. The only difference between the phases of a multiphase buck converter is the physical resistance of the phases i.e. Req. It will be shown in the chapter on hardware development that because of the layout of the MOSFET devices as well as the physical construction of the inductors of the phases, it is inevitable that small differences will appear in the values of Req. This difference in the values of equivalent series resistances of the phases will contribute to small differences in the estimated currents and corresponding phase duty cycles. The simulation of the above derived equations is carried out in MATLAB/ SIMULINK devices and the results will be presented in a later chapter.

18

CHAPTER 4: CURRENT CONTROL OF MULTIPHASE BUCK CONVERTER

The multiloop control structure adopted for the control of four phase buck converter in this work consists of two loops: outer MPPT/ voltage control loop and inner current control loop. The focus of this chapter is the predictive current programmed control method adopted of the inner current control loop of the multiphase buck converter.

4.1 Predictive Current Control of Buck Converter

Predictive current programmed control method adopted in this work is presented in [20]. The predictive control method essentially employs the model of the plant in order to derive the control law. The foremost advantage of this type of control method is that the control law is derived from the mathematical model of the very plant which is to be controlled. No gain adjustments or controller parameter derivations are required. This type of control method is very intuitive and easy to understand. Moreover, the control law is derived in discreet domain which makes it ideally suitable for implementation on a digital signal processor.

The inductor current waveform for two consecutive switching cycles is analyzed next in order to derive the predictive current control law for single phase buck converter.
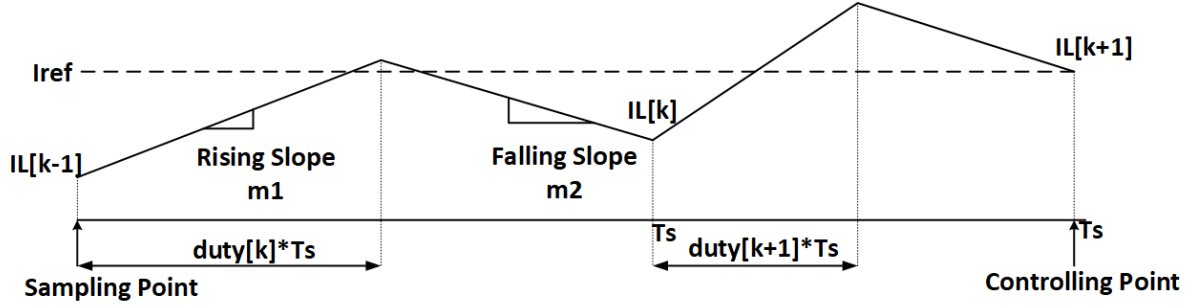
Figure 4.1 Inductor current waveform for two switching cycles

The inductor current waveform for two switching cycles is shown in **Figure 4.1**. It should be mentioned that the input voltage Vin and output voltage Vout are assumed to be essentially constant during these two switching cycles. This assumption is valid because switching period for the dc-dc converter is very small.

The inductor current at the end of kth cycle i.e. IL[k] can be written in terms of the inductor current at the beginning of the switching cycle i.e. IL[k-1] and the rising and falling slopes m1 and m2 respectively.

$$IL[k] = IL[k-1] + m1[k] * duty[k] * Ts + m2[k] * duty'[k] * Ts$$

(4.1)

The values of the inductor current rising and falling slopes during one switching period were derived in previous chapter as Equation 3.5 and Equation 3.6 and are reproduced here:

$$m_1[k] = \frac{V_{in}[k] - I_L[k] * R_{eq} - V_{out}[k]}{L}$$

(4.2)

$$m_2[k] = \frac{- I_L[k] * R_{eq} - V_{out}[k]}{L}$$

(4.3)

Where Req is defined in Chapter 3.

We replace the values of m1[k] and m2[k] into Equation 4.1 and simplify to obtain following:

20

$$IL[k] = IL[k-1] * \left(1 - \frac{R_{eq} * Ts}{L}\right) + \frac{Vin[k] * duty[k] * Ts}{L} - \frac{V_{out}[k] * Ts}{L} \quad (4.4)$$

Here the fact that duty[k]+duty'[k]=1 has been used. For simplification purposes, we can define a new parameter 'a' as:

$$a = 1 - \frac{R_{eq} * Ts}{L} \quad (4.5)$$

Now rewriting Equation 4.4 as:

$$IL[k] = IL[k-1] * a + \frac{Vin[k] * duty[k] * Ts - V_{out}[k] * Ts}{L} - \frac{V_{out}[k] * Ts}{L} \quad (4.6)$$

Equation 4.6 can be extended to the next switching cycle as follows:

$$IL[k+1] = IL[k] * a + \frac{Vin[k] * duty[k+1] * Ts}{L} - \frac{V_{out}[k] * Ts}{L} \quad (4.7)$$

It should be noted that the input voltage and the output voltage are taken to be the same in the next switching cycle as well. This is based on the assumption that the dc input and output voltages remain essentially constant during very short time period of two consecutive switching cycles. The duty cycle duty[k+1] is the variable of interest to be calculated in the present switching cycle and applied at the beginning of the next switching cycle. The value of IL[k+1] is the reference current value as depicted in Fig. 4.1. Next the value of IL[k] is replaced in Equation 4.7 from Equation 4.6 and simplification is carried out.

$$\begin{aligned} IL[k+1] = IL[k-1] * a^2 &+ \frac{Vin[k] * duty[k+1] * Ts}{L} \\ &+ \frac{Vin[k] * duty[k] * Ts * a}{L} - \frac{2 * V_{out}[k] * Ts}{L} \end{aligned} \quad (4.8)$$

We need to calculate the value of duty cycle for the next switching cycle i.e. duty[k+1]. Therefore, we rearrange the Equation 4.8 as follows:

$$duty[k + 1] = \frac{L}{Vin[k] * Ts} * (Iref - IL[k - 1] * a^2) - a * duty[k]$$
$$- \frac{2 * V_{out}[k]}{Vin[k]}$$

(4.9)

The Equation 4.9 is used to implement the predictive current control in this work. It should be noted that if the converter parasitics are ignored, i.e. Req = 0, then Equation 4.9 reduces to the equation presented in [20].

4.2 Extension to Multiphase Version

The Equation 4.9 is derived for the single phase buck converter. However, the same equation can be used to calculate duty cycles for the multiple phases of four phase buck converter as well. We can extend the Equation 4.9 as follows:

$$dutyn[k + 1] = \frac{L}{Vin[k] * Ts} * (Iref - ILn[k - 1] * a^2) - a * dutyn[k]$$
$$- \frac{2 * V_{out}[k]}{Vin[k]}$$

(4.10)

It should be noted here that the estimated currents and the calculated duty cycles for the four phases will differ only because of the different practical values of series equivalent resistances of the phases. This difference will be highlighted further in the chapter describing hardware development of prototype converter.

CHAPTER 5: MPPT AND BATTERY CHARGING CONTROL

The major focus of this work is the sensorless predictive current control of a multiphase buck converter. This converter is intended to be used as an alternative to the commercially available solar MPPT charge controllers. The control structure adopted consists of two loops; inner current control loop which is discussed in the previous chapters and outer MPPT/ battery charging control loop which is the topic of discussion in this chapter.

The solar charge controller is connected to the array of solar panels known as PV array and the output of such a converter system is connected to a lead acid or lithium Ion battery for energy storage applications. Such a converter can be used to power DC loads directly as well. The main objective of MPPT solar charge controller is to extract maximum power from the connected PV array and charge the connected battery bank in a controlled and efficient manner. This implies that the charging voltage and charging current of the connected battery pack should be regulated by the MPPT solar charge controller.

The outer loop of the dual loop structure has two separate objectives:

- Extract maximum power from PV array using suitable algorithm
- Control the charging of the connected battery bank and ensure safe limits of voltage and current for the battery pack

In this chapter, the MPPT algorithm adopted in this work is discussed first. Then the charging scheme adopted for the battery charging is discussed.

5.1 Hill Climbing MPPT Algorithm

In order to understand the working of MPPT algorithm, first we present the electrical characteristics of the PV array as presented in [22].
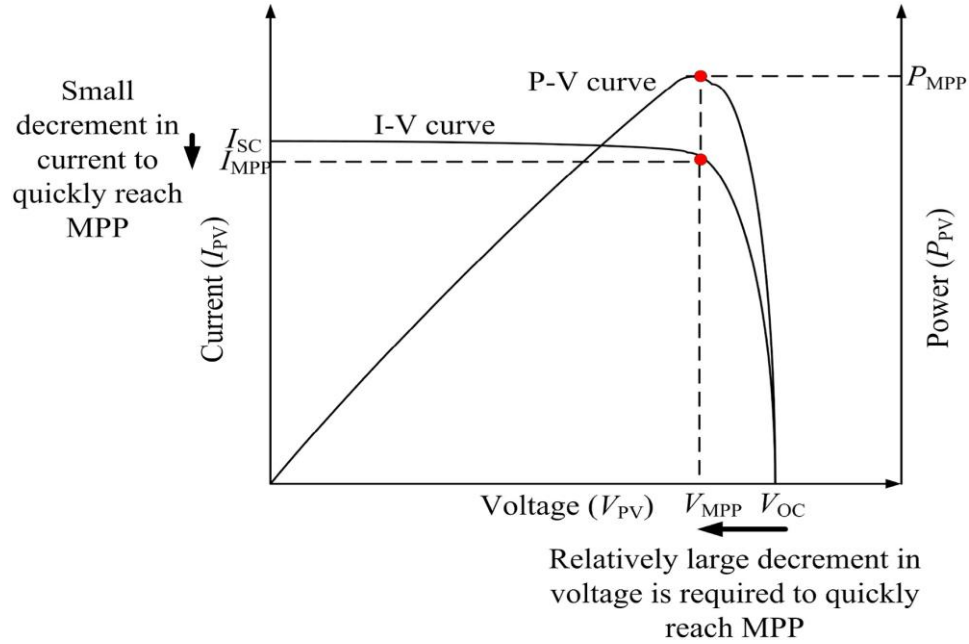

Figure 5.1 PV Array characteristic curve

As can be seen in **Figure 5.1**, the power voltage curve of the PV array resembles that of a hill. In order to reach the maximum power point (Pmpp) of the PV array, the converter needs to climb the hill from either side of the maximum power point. The class of algorithms that takes into account this very nature of P-V curve in order to reach the Pmpp is known as hill climbing algorithms.

There are many variations of the hill climbing algorithm presented in literature as presented in [22]. Since the focus of this work is on the sensorless predictive current control of a multiphase buck converter, we have adopted a simple and easy to implement variation for demonstration purposes in this work. The hill climbing algorithm adopted is known as Perturb and Observe (P&O) method and is presented in next section.

24

5.1.1 Perturb and Observe MPPT Algorithm

In P&O algorithm, the operating point of the converter is disturbed or changed purposefully in order to perturb the power being drawn from the PV array. The new power level is compared with the previous power level and the direction of next perturbation is determined. If the power increases, the next perturbation is carried out in the same direction, otherwise the perturbation is carried out in the opposite direction. The flowchart of the algorithm is presented next.
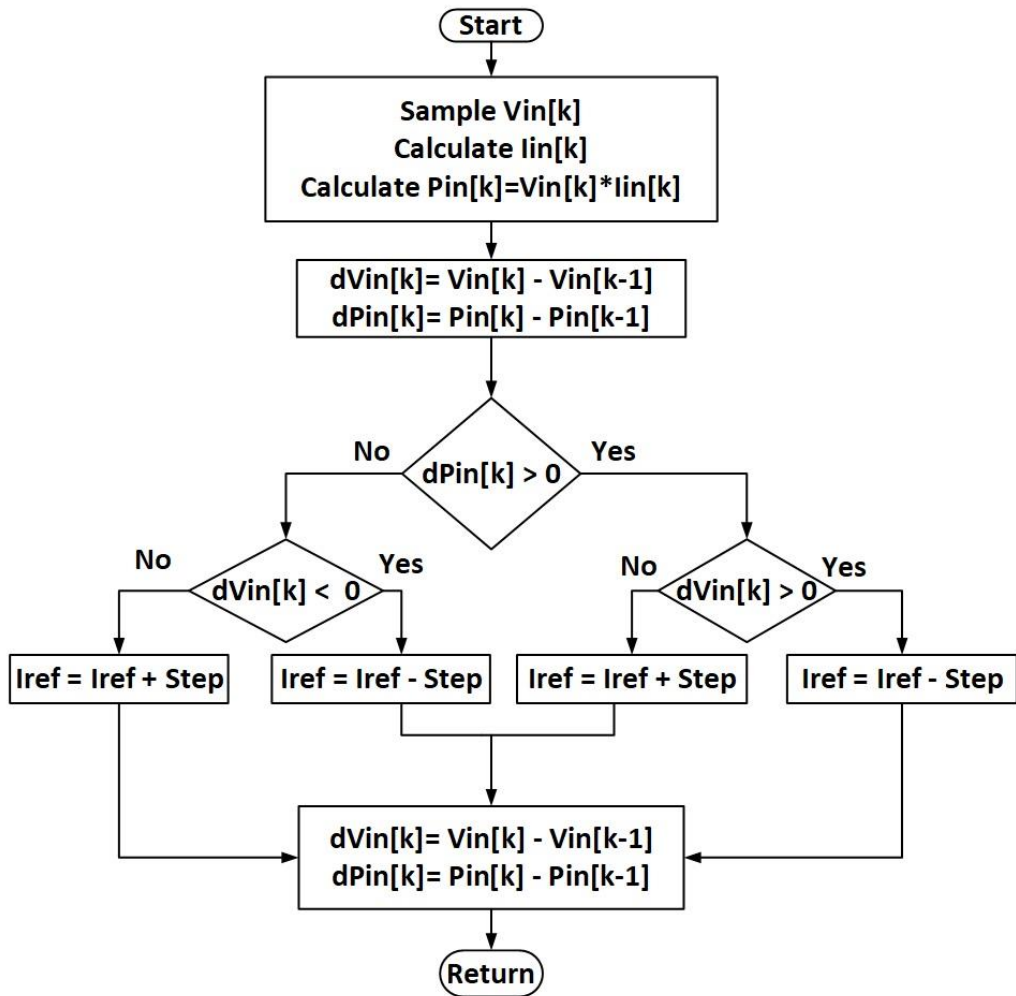
Figure 5.2 P&O algorithm for MPPT tracking

The algorithm in **Figure 5.2** calculates the PV array current and the PV array power at the start of current iteration whereas the only variable sampled is input voltage i.e. PV array voltage. The input current of a buck converter is simply related to the output current or the inductor current as follows:

$$Iin[k] = IL[k] * duty[k] \qquad (5.1)$$

The above expression is for single phase version. In case of a multiphase buck converter, the input current is simply the sum of all the currents reflected to the input as follows:

$$Iin[k] = IL1[k] * duty1[k] + IL2[k] * duty2[k] + \cdots \qquad (5.2)$$

The input PV array power is then simply the product of input voltage and input current. The slope of the P-V curve is determined next. The derivatives of the input power and input voltage are calculated and used to determine the direction of the next perturbation. It should be noted that the control variable for the MPPT loop as shown in **Figure 5.2** is the reference current for the inner current control loop and not the duty cycle of the converter as is conventionally the case. The reason is the dual loop control structure for the multiphase buck converter adopted in this work. The MPPT loop perturbs the operation point of the converter and thus the PV array power by changing the reference current of the inner current control loop. In this work, a simple constant step size for the reference current is used to keep implementation simple. Further details on the algorithm can be found in [22]. The simulation results of the algorithm are presented in the next chapter.

5.2 Battery Charging Control

The target application of multiphase buck converter presented in this work is commercial MPPT solar battery charge controller. The task of these devices is to extract maximum power from the PV source and charge the connected battery bank as well as provide power to the connected loads. Battery charging control is thus an integral function of these devices.

Numerous battery charging methods have been presented in the literature [25]. They are classified according to the types of different battery technologies they are developed for. In this work, a simple constant current constant voltage charging method is adopted. In this method, the battery is charged at a constant current value which is typically C/10 or C/20, where 'C' stands for the battery capacity, until the battery terminal voltage reach the maximum charge voltage. After that, battery terminal voltage is maintained constant at that level by the converter. The algorithm is presented in the following flowchart.
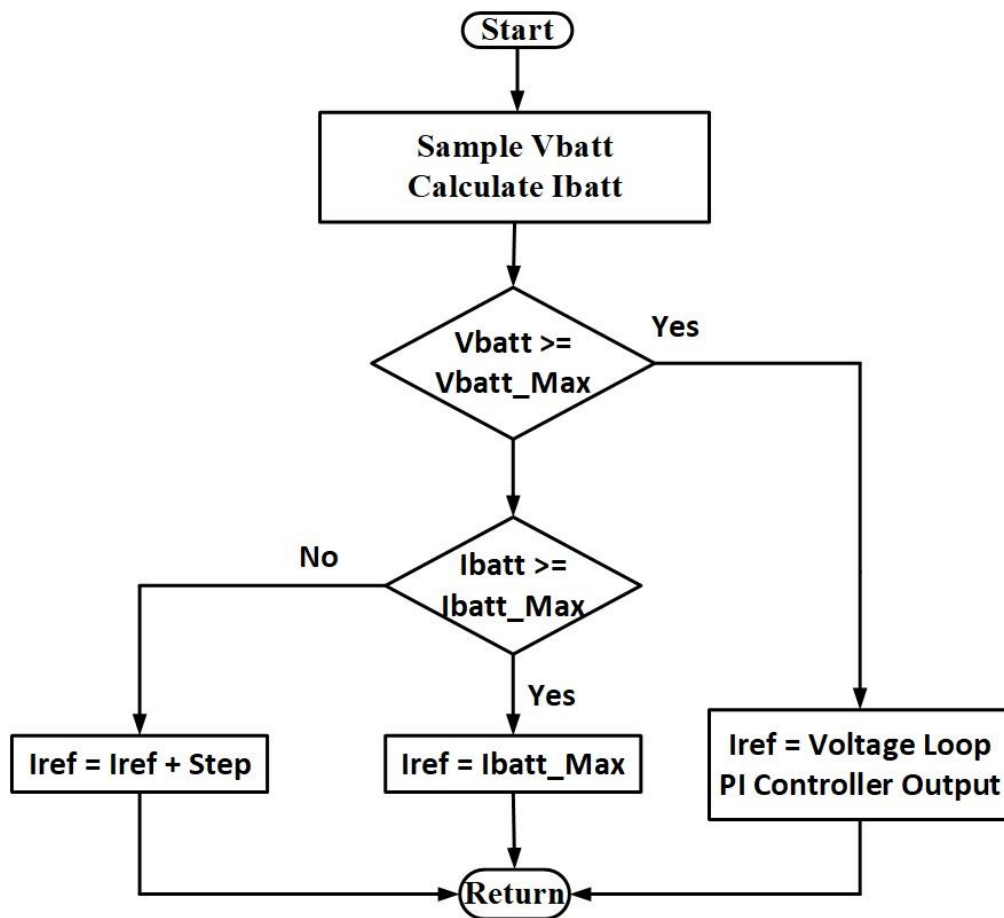
Figure 5.3 Battery Charging CC-CV algorithm

As can be seen in **Figure 5.3**, the algorithm first determines if the battery voltage is less than the maximum battery voltage threshold. If the voltage is less that maximum permissible voltage, this means the battery has the capacity to accept bulk charge. The battery is therefore charged at maximum possible current until the battery current reaches

27

its maximum threshold. After that, the Iref of the converter is maintained at its maximum value. It should be noted that this algorithm assumes that no dc load is connected at the output and the entire converter current is being fed into the battery. If DC load is indeed connected, then one current sensor is indispensable in order to differentiate between the battery current and DC load current.

When battery voltage reaches its maximum value, the value of Iref or the converter is determined by the PI controller employed in the voltage loop. This is a simple PI controller whose output is the reference current for the inner current control loop. The MATLAB/SIMULINK implementation results are shared in the next chapter.

CHAPTER 6: MATLAB / SIMULINK SIMULATION RESULTS

The main focus of this work has been the sensorless current control of a four phase buck converter. The dual loop control structure adopted for the control of the four phase buck converter consisted of two loops: an outer loop that performs MPPT tracking of the solar array as well as battery charging control and an inner current control loop. The theoretical formulation of both the control loops has been developed in the previous chapters. In this chapter, we provide the details regarding the simulation of the four phase buck converter as well as the control system.

6.1 Four Phase Buck Converter

The four phase buck converter consists of four parallel buck converter stages which share a common input and output bus. We simulate the four phase buck converter power stage in MATLAB/ Simulink environment as this software is available for academic use.
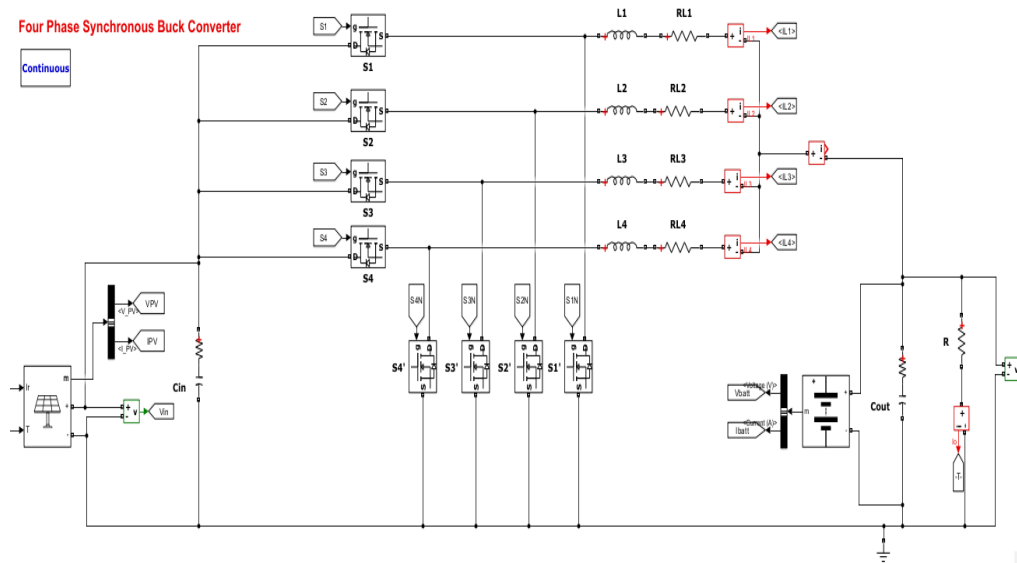
Figure 6.1 Four phase buck converter power stage

The specification of the four phase buck converter as it is simulated in SIMULINK can be summarized as follows:

**Table 6.1** Parameters of four phase buck converter

S. No.	Parameter	Value
1	Input Voltage	30 V
2	Output Voltage	14 V
3	Maximum output current	20 A
4	Switching frequency	100 KHz
5	L1, L2, L3 and L4	200 uH
6	RL1, RL2, RL3 and RL4	10 mΩ
7	Rds1, Rds2, Rds3 and Rds4	1 mΩ
8	Cin and Cout	220 uF

The converter parasitics are modeled by series resistances of the MOSFET switches (Rds) and equivalent series resistances of the inductors (RL). The sum of these two values is the equivalent series resistance of each phase Req as described in Chapter 3.

It should be noted in **Figure 6.1** that PV array source and battery bank are attached at the input and output of the converter as these are the real sources the converter is supposed to work with. Next we present the simulation results for the inner current control loop as well as outer MPPT/ voltage control loop.

6.2 Current Control Loop

The inner current control loop performs two functions: it estimates the inductor current by sampling the input and output voltages and then controls this estimated current. In order to test the performance of the current estimation and current control, we disable the outer loops and simulate the inner current control loop with a fixed reference current command of 2 A. The simulation results are presented for one phase next.
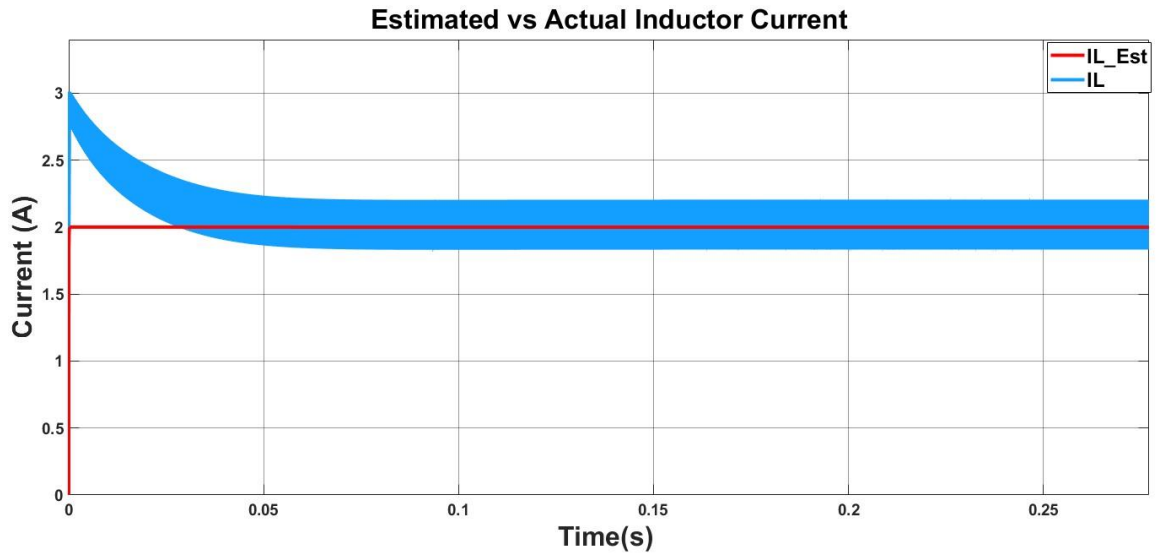
Figure 6.2 Estimated vs Actual Inductor currents for one phase, Iref = 2A

As can be seen from **Figure 6.2**, the estimated inductor current is controlled by inner current control loop successfully. It should be noted that the actual inductor current exhibits overshoot before converging to the estimated current value. The current control loop actually controls the estimated current and not the actual current. As soon as the transients die out, the actual inductor current converges to the estimated and controlled value. It should also be noted that the outer voltage loop is disabled in this example. Next we present the steady state waveforms of all the four phase currents.
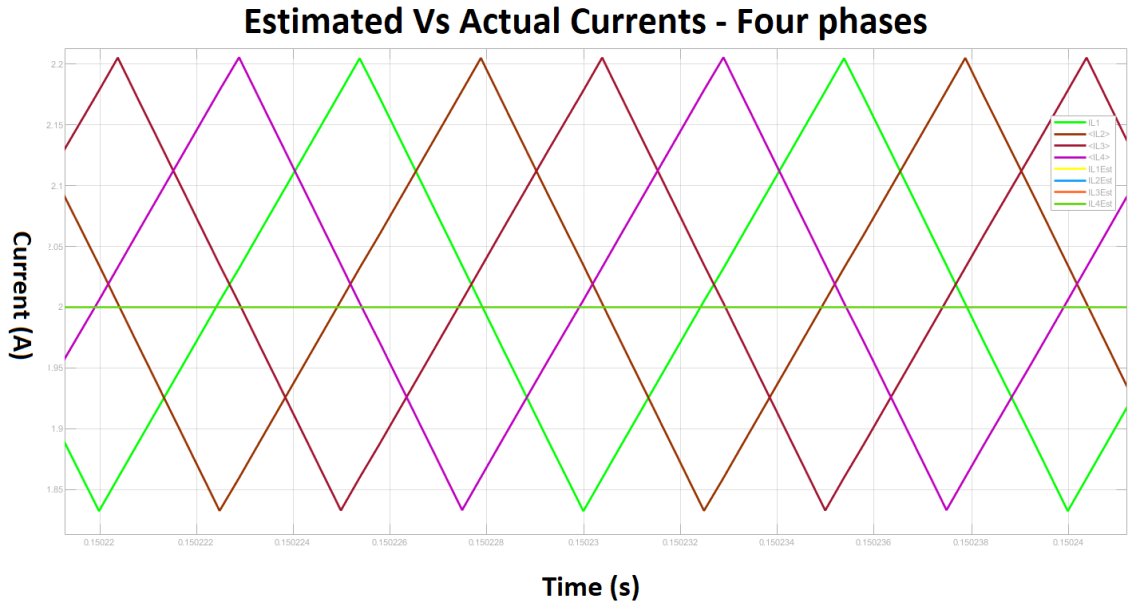
Figure 6.3 Four phase currents

As can be seen in **Figure 6.3**, the four phase currents of the multiphase buck converter converge on the estimated and controlled values of their phases.

6.3 Voltage Loop Control

The current loop control of four phase buck converter is shown to perform well in the previous section. In this section, we present the simulation results of the outer voltage loop of the dual loop control structure. First, only output voltage control is activated to achieve the constant voltage at the output of the multiphase buck converter.
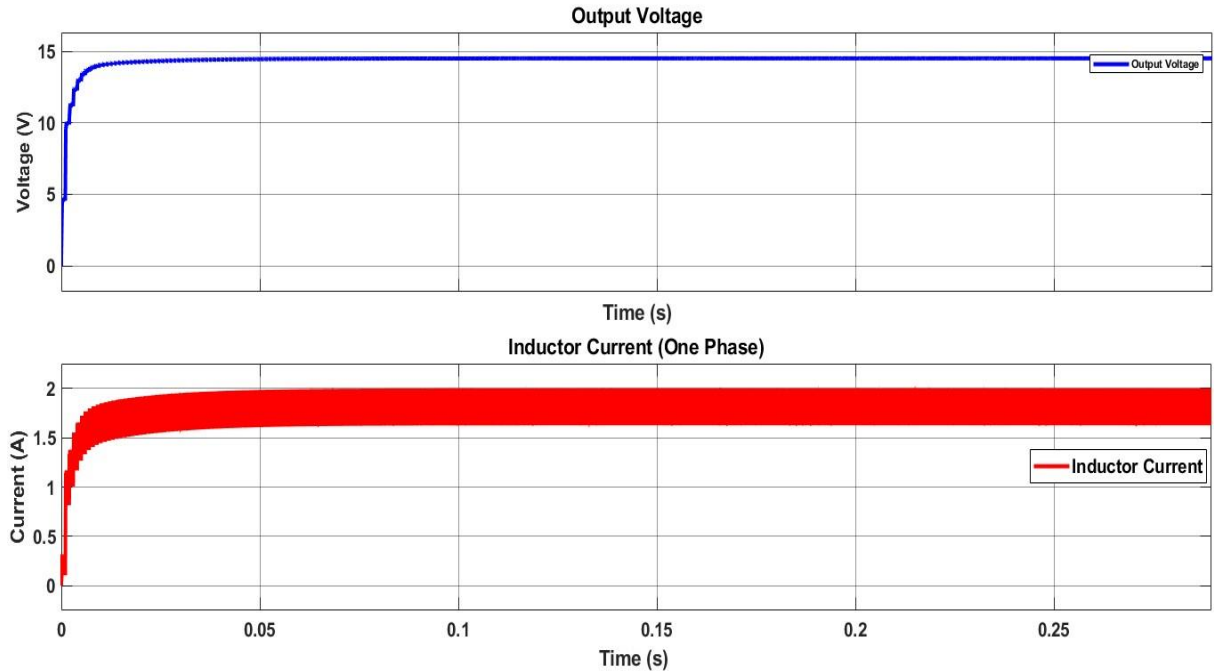
Figure 6.4 Voltage and phase current - Dual loop control

The voltage loop controller is a simple PI controller. The gains of PI controller are selected by inspection of the loop response in simulation. It can be seen that the voltage rises in the steps until it reaches the steady state value. This is because the voltage loop is executed at a slower pace than the inner faster current control loop.

6.4 MPPT Control Loop

In this section, we present the simulation results of the MPPT tracking by the four phase buck converter. In order to simulate the MPPT tracking, we connect a PV array block at the input of the converter and also connect a Lead Acid type battery pack at the output of the converter. Next we present the power output from the solar array.
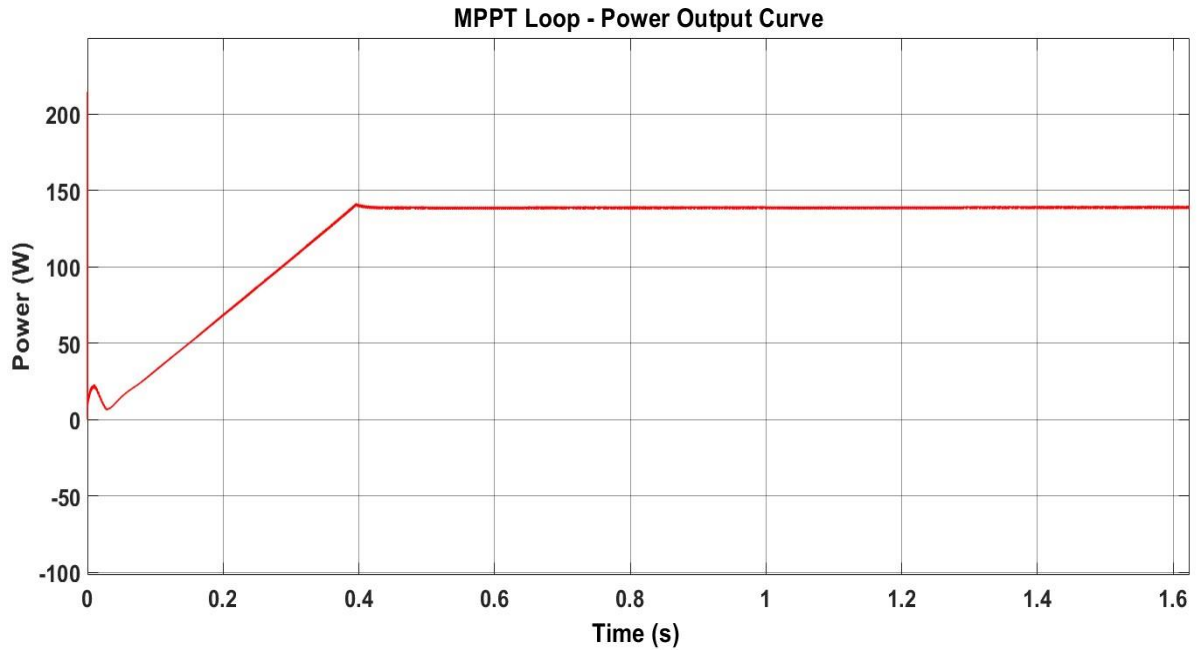
Figure 6.5 Power output from PV array - MPPT tracking

As can be seen in **Figure 6.5**, the power output from the PV array steadily increase during MPPT tracking. The algorithm is able to extract almost 145 watts from a maximum power point of 150 watts. This equals MPPT tracking efficiency of almost 97%. Next we present the battery voltage connected at the output of the converter as well as the phase current and input voltage progression during the MPPT tracking working.
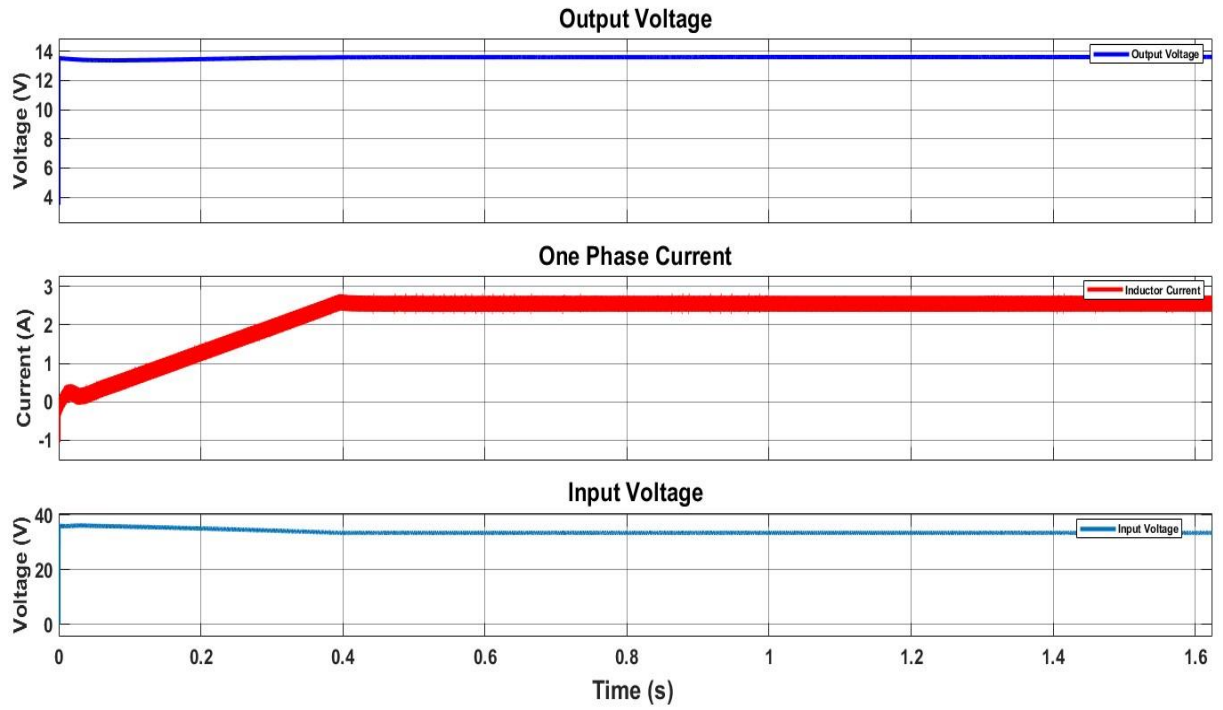
Figure 6.6 Battery Voltage, Phase Current, Input Voltage - MPPT Tracking

As can be seen, the waveforms show steady progression during the working of the MPPT tracking algorithm.

CHAPTER 7: HARDWARE DEVELOPMENT

The theoretical background of the dual loop control structure adopted for four phase buck converter has been developed in the previous chapters. The current estimation and current control loop equations were derived as well as the outer voltage and MPPT tracking loop were discussed. The simulation of the above mentioned loops with the four phase buck converter power stage is carried out in MATLAB/ SIMULINK environment and the simulation results presented in the last chapter. In order to study the practical implementation of the above mentioned sensorless current control scheme for a four phase buck converter, a hardware prototype has been developed. This chapter describes the motivation, development and the issues faced regarding the working of a hardware prototype.

7.1 Motivation

The majority of the MPPT tracking solar charge controllers available in the market are of single phase buck type. An example is shown below [27]:


Figure 7.1 Commercial MPPT charge controller

The example cited above in **Figure 7.1** Commercial MPPT charge controller is a 60 A version. The large size of the converter can be attributed to the large size of the magnetics used. In fact, the magnetic element is embedded in the large body heat sink. In order to develop a better product at a comparable cost, it was undertaken to explore the possibility of adopting a multiphase design for the commercial MPPT market.

7.2 Hardware Layout

In this work, a four phase buck converter hardware prototype is developed in order to act as a test-bed for the implementation of sensorless current control scheme. The layout of the hardware is shown next:
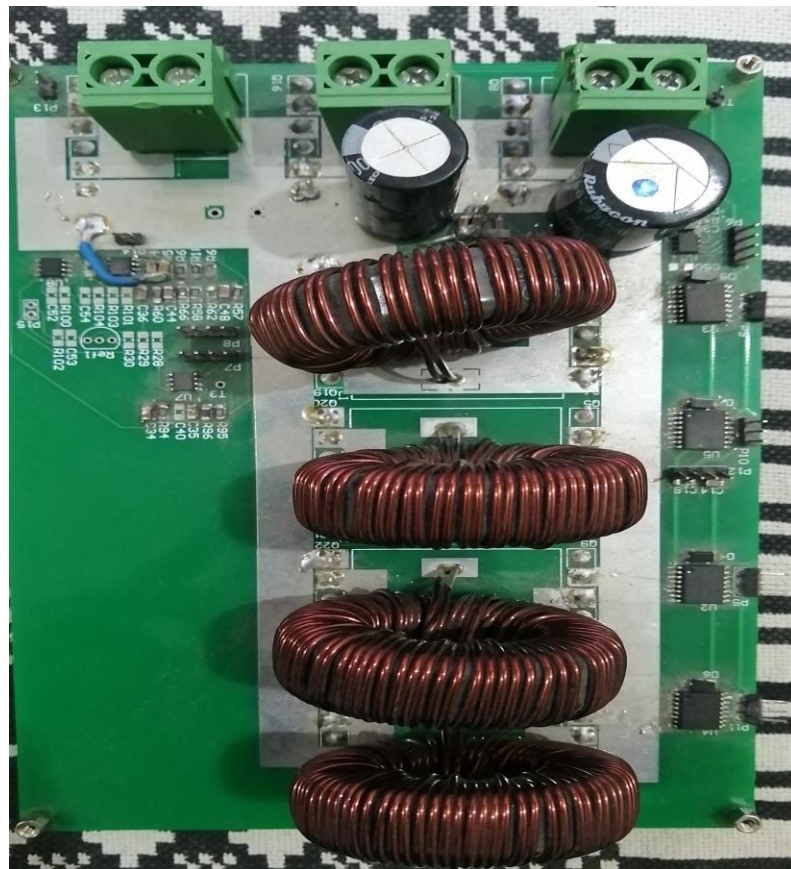
Figure 7.2 Four phase buck converter – Hardware

As can be seen in **Figure 7.2** Four phase buck converter – Hardware, the four phases of the buck converter are placed in a cascaded manner. This will introduce a difference in the equivalent series resistance of the phases and can introduce errors in current estimation and control if same value for equivalent series resistance is assumes. Therefore, a calibration method must be used. One possible method is to turn individual phase ON with rest of the phases OFF and then measure the input and output voltages. With the value of the test load connected at the output known, equivalent series resistance can be calculated as follows:

$$Vout = Vin * duty - ILn * Reqn$$

(7.1)

It should be noted that the values of input and output voltages in the above equation are average values and can be calculated by using a low pass filter after ADC results. The duty cycle should be kept constant at a given value. The value of the dc inductor current is given as:

$$ILn = \frac{Vout}{Reqn}$$

(7.2)

Therefore, the value of the Req for each individual phase can be determined easily. It should be noted that the Req determined using the practical values of input and output voltage will include the parasitic resistance introduced by the PCB traces.

The hardware prototype assembled consists of four phases of buck converter. The four phases share single input and output rails which are made by single electrolytic capacitors are shown. The power devices are assembled on the lower side of the PCB in order for direct connection with the heat sink base plate. This is shown in following figure.
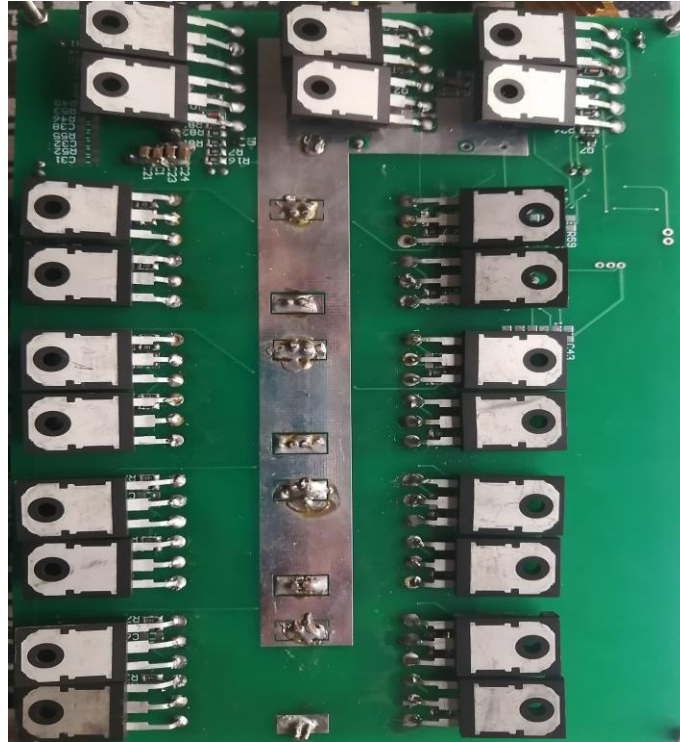
Figure 7.3 Power devices of four phase buck converter hardware prototype

The connectors used for input and output connections are of high power type. The auxiliary power supply for the gate drivers and sensing circuits is implemented off board in the initial version.

7.3 Controller Implementation – STM32G474

The current estimation and control algorithm is derived in discreet domain. The actual implementation of the sensorless current control is completely digital in nature. Therefore, a special digital signal processor STM32G474 from STM32G4 series from ST Microelectronics is selected to implement the current estimation and current control.
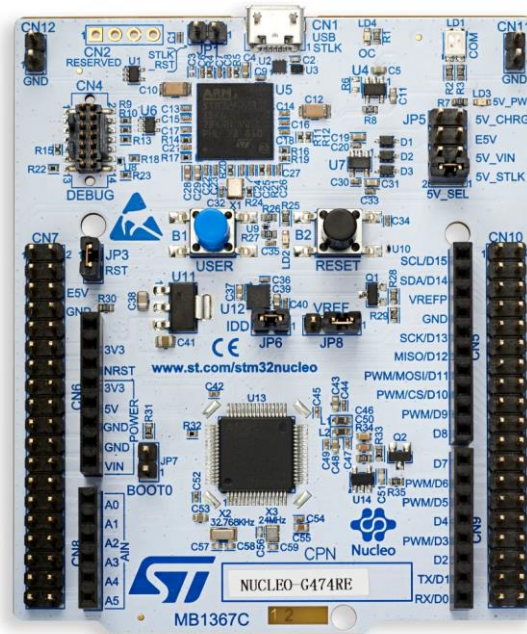
Figure 7.4 STM32G474 development board

The STM32G4 series is specially designed for Power Electronics applications. The device incorporates a special high resolution timer unit for generating multiple PWM waveforms for the multiphase applications. The device also incorporates high speed ADC which are crucial in sensing the real world analog signals. The processor is capable of 170 MHZ operation which enables the device to perform the mathematical operations in time constrained applications. The current estimation and control are implemented in the Interrupt service routine of the Timers. The algorithm sequence can be described as follows:
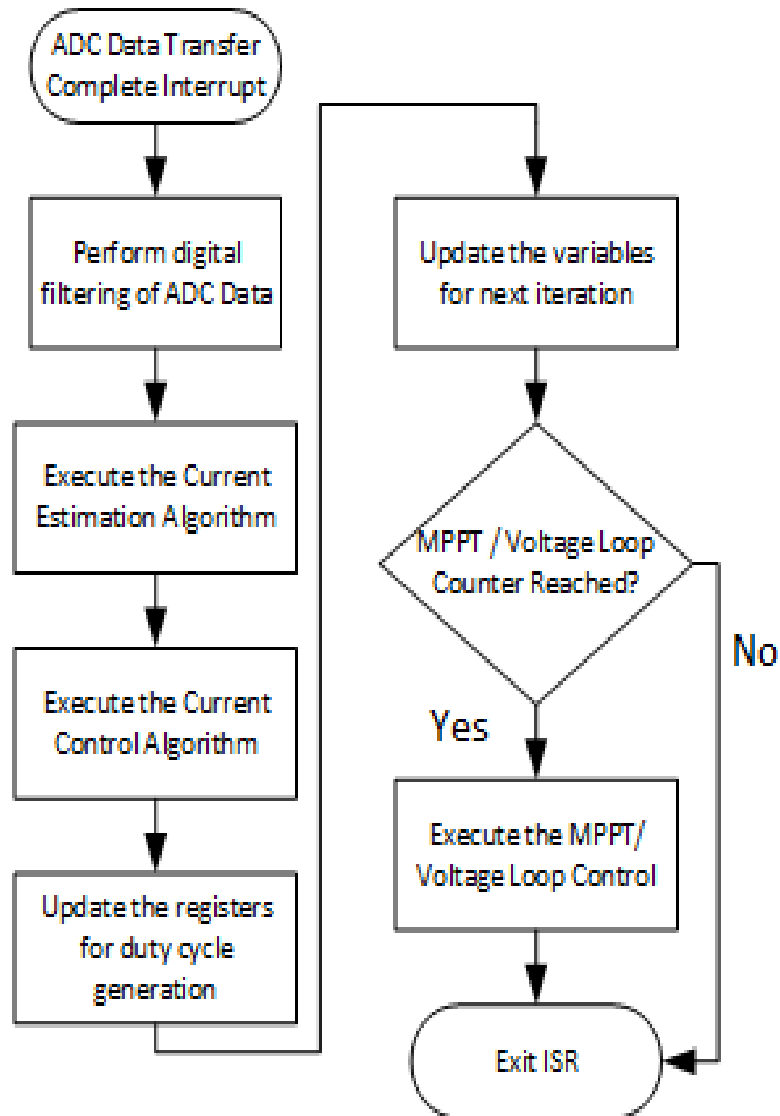
Figure 7.5 Software Algorithm

As can be seen, the current estimation and current algorithm are implemented at each switching cycle. The execution frequency of inner current estimation and current control loop is equal to the switching frequency. The outer MPPT / voltage control loop is executed at much slower frequency and their execution is controlled by a simple counter mechanism.

The software for the STM32G474 device is written in C language which is industry standard for embedded system applications. The C language offers speed and ease programming as compared to other alternatives such as assembly language. The software

development environment used for programming and testing the hardware peripherals such as PWM and ADCs is STM32Cube IDE environment. This is a free of cost software provided by STM for development of STM devices and controllers. The software is written and compiled in STM32Cube IDE shown below:
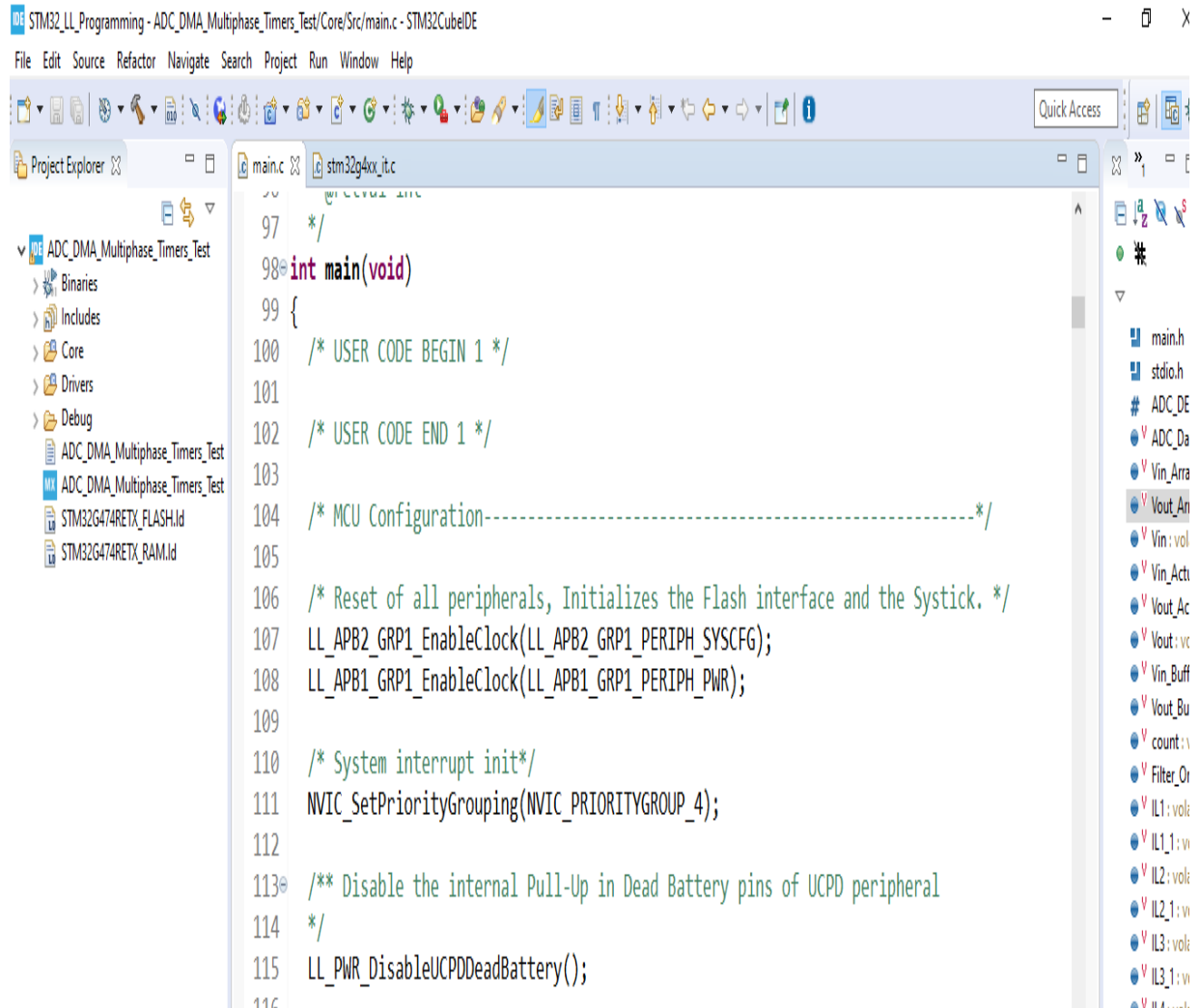
Figure 7.6 STM32 Cube IDE

7.4 Prototype Working and Issues Encountered

The hardware prototype is assembled and is made to work in open loop successfully. Unfortunately, the actual implementation of the sensorless current control algorithm on the hardware has not been possible due to following issues.

- The input and output voltages need to be sampled at the switching frequency.
- The hard switched converter waveforms contain significant switching noise. This noise made the ADC reading unstable and the values of these variables could not be sampled successfully inside the digital controller.

The author unfortunately lacks the know-how and expertise to implement the ADC interface circuitry that can make the sampling of the converter input and output voltages possible.

Due to above mentioned reasons, the current state of the prototype development is at open loop working only. In future, the hardware prototype will be revised, hopefully with better know how and technical expertise so as to successfully achieve ADC sampling.

CHAPTER 8: CONCLUSION

In this work, sensorless current control of a four phase buck converter has been presented. The converter is targeted for MPPT tracking battery charging applications. The dual loop control structure has been adopted and demonstrated for the converter. The controller consists of two loops, outer MPPT/ battery control loop and inner current control loop. The outer loop controls the tracking of the power from PV panels as well as battery charging and sets the reference for the inner current control loop. The inner current control loop estimates the inductor currents and then controls the currents to track the reference value. The entire control system is simulated along with power stage in MATLAB/ SIMULINK environment and the simulation results co relate with the theoretical formulations.

A hardware prototype development is attempted and its construction and working is briefly explained. Issues encountered in the close loop working of the hardware prototype have been explained. Future work will continue on improving the hardware prototype.

REFERENCES

[1] P. T. K. P. M. a. M. F. Greuel, "Sensorless current mode control-an observed-based technique for dcdc converters," *IEEE IEEE Transactions on Power Electronics,* vol. 16, no. 4, pp. 522-526, 2001.

[2] P. Mattavelli, "Digital control of dc-dc boost converters with inductor current estimation," in *Nineteenth Annual IEEE Applied Power Electronics Conference and Exposition*, Anaheim, CA, USA, 2004.

[3] A. G. Beccuti, "Explicit model predictive control of dc–dc switched-mode power supplies with extended kalman filtering," *IEEE Trans. Ind. Electron,* vol. 56, no. 6, p. 1864–1874, 2009.

[4] Q. e. Tong, "A sensorless predictive current controlled boost converter by using an ekf with load variation effect elimination function," *Sensors,* vol. 1, no. 1, p. 9986–10 003, 2015.

[5] e. M. H. Cervantes, "Real-time simulation of a luenberger observer applied to dc-dc converters," *IEEE Latin America Transactions,* vol. 16, no. 3, pp. 981-986, 2018.

[6] H. L. Y. Q. a. X. Chen, "Digital average current-mode control of pwm dc–dc converters without current sensors," *IEEE Transactions on Industrial Electronics,* vol. 57, no. 5, pp. 1670-1677, 2010.

[7] e. X. Zhang, "Sensorless current sharing in digitally controlled two-phase buck dc-dc converters," in *Twenty-Fourth Annual IEEE Applied Power Electronics Conference*, Washington, DC, USA, 2009.

[8] Z. Lukic, "Digital controller for multi-phase dc-dc converters with logarithmic current sharing," in *IEEE Power Electronics Specialists Conference*, Orlando, FL, USA, 2007.

[9] M. Duan, "Sensorless current-sharing scheme for multiphase dc-dc boost converters," *IEEE Transactions on Power Electronics,* vol. 38, no. 2, pp. 1398-1405, 2023.

[10] M. R., "An optimal current observer for predictive current controlled buck dc-dc converters," *Sensors,* vol. 1, no. 1, p. 8851–8868, 2014.

[11] Wang, "Research on valley current prediction control algorithm based on buck converter," *Journal of Physics: Conference Series,* vol. 1, no. 1, 2010.

[12] G. Cimini, "Robust current observer design for dc-dc converters," *Sensors,* vol. 1, no. 1, p. 8851–8868, 2014.

[13] K. D. M. Bayimissa, "Performance evaluation of voltage and current control mode controller for sepic converter in cubesats application," in *International Conference on the Industrial and Commercial Use of Energy (ICUE)*, Cape Town, South Africa, 2015.

[14] S. H. a. R. M. Nelms, "Comparison of three implementations of digital average current control for dc-dc converters," in *IECON 2014 - 40th Annual Conference of the IEEE Industrial Electronics Society*, Dallas, TX, USA, 2014.

[15] E. Bianconi, "Perturb and observe mppt algorithm with a current controller based on the sliding mode," *International Journal of Electrical Power and Energy Systems,* vol. 1, no. 1, p. 346–356, 2013.

[16] T. K. V. H. C. a. J. E. Kim, "Design and control of proportional-resonant controller based photovoltaic power conditioning system," in *IEEE Energy Conversion Congress and Exposition*, San Jose, CA, USA, 2009.

[17] H. H. Lee, "The space vector pwm for voltage source inverters using artificial neural networks based on fpga," *International Forum on Strategic Technology,* vol. 1, no. 1, p. 396–401, 2010.

[18] C. Restrepo, "Improved model predictive current control of the versatile buck-boost converter for a photovoltaic application," *IEEE Transactions on Energy Conversion,* vol. 37, no. 3, p. 1505–1519, 2022.

[19] C. R. a. J. M. C. R. B. P. Cáceres, "Finite control set model predictive current control of the coupled-inductor buck–boost dc–dc switching converter," in *IEEE International Conference on Automation/XXIII Congress of the Chilean Association of Automatic Control (ICA-ACCA)*, Concepcion, Chile, 2018.

[20] A. P. a. D. M. R. W. E. Jingquan Chen, "Predictive digital current programmed control," *IEEE Transactions on Power Electronics,* vol. 18, no. 1, pp. 411-419, 2003.

[21] H. M. a. S. K. Kobayashi, "An excellent operating point tracker of the solar-cell power supply system," *IEEE Trans. Ind. Electronics,* vol. 53, no. 2, pp. 495-499, 2006.

[22] e. Vibhu Jately, "Experimental analysis of hill-climbing mppt algorithms under low irradiance levels," *Renewable and Sustainable Energy Reviews,* vol. 150, no. 1, p. 495–499, 2021.

[23] L. Shang, "An improved mppt control strategy based on incremental conductance algorithm," *Protection and Control of Modern Power Systems,* vol. 5, no. 14, pp. 123-127, 2020.

[24] P. Krein, "Ripple correlation control, with some applications," *IEEE ISCAS,* vol. 5, no. 1, p. 283–286, 1999.

[25] A. A.-H. Hussein, "A review of charging algorithms for nickel and lithium battery chargers," *IEEE TRANSACTIONS ON VEHICULAR TECHNOLOGY,* vol. 60, no. 3, 2011.

[26] D. M. a. R. W. Erickson, Fundamentals of Power Electronics, USA: Springer Cham, 2001.

[27] EPEVER, *EPEVER tracer 60 A charge controller,* China: China, 2023.